Low Temperature Physics/Fizika Nizkikh Temperatur, 2021, vol. 47, No. 2, pp. 159–172

Theory of the shear acoustic phonons spectrum and their interaction with electrons due to the piezoelectric potential in AlN/GaN nanostructures of plane symmetry

I. V. Boyko and M. R. Petryk

Mathematical Modeling of Mass Transfer Laboratory, Ternopil Ivan Puluj National Technical University
Ternopil 46001, Ukraine
E-mail: boyko.i.v.theory@gmail.com
Mykhaylo_Petryk@tntu.edu.ua

J. Fraissard

Sorbonne Universités, ESPCI-LPEM, 10 rue Vauquelin, Paris F-75231, France
E-mail: jacques.fraissard@sorbonne-universite.fr

Received October 6, 2020, published online December 25, 2020

Using the models of elastic and dielectric continuum the system of differential equations is obtained, the exact analytical solutions of which describe the elastic displacement of the medium for nitride-based semiconductor nanostructure and the piezoelectric effect, which is caused by shear acoustic phonons. The theory of the shear acoustic phonons spectrum and caused by them piezoelectric potential were developed. It is shown that shear acoustic phonons do not interact with electrons due to the deformation potential, but such interaction can occur due to the piezoelectric potential. Using the method of temperature Green's functions and Dyson equation, expressions that describe the temperature dependences of the electronic levels shifts and their decay rates are obtained. Calculations of the spectra of electrons, acoustic phonons, and characteristics that determine their interaction at different temperatures were carried out using the example of physical and geometric parameters of typical AlN/GaN nanostructure, which can function as an element of a separate cascade of a quantum cascade laser or detector.

Keywords: acoustic phonon, nitride-based semiconductor, piezoelectric effect, Dyson equation, Green's function.

1. Introduction

The operation of modern quantum cascade detectors [1] and lasers [2] of the middle and far range electromagnetic waves substantially depends on polarization effects in nitride-based semiconductors, which serve as material for the layers of these nanodevices cascades. The most substantial is the effect of a strong internal field [3] caused by spontaneous [4, 5] and piezoelectric polarizations [6]. Besides, different values of the total polarization at the boundaries of the nanostructure layers give rise to charges at these heterointerfaces. This effect, as well as the presence of a dynamic charge in nanostructures caused by the gradient of acceptor impurities in the nanostructure, is the main difficulty in the development of theoretical methods for calculating the energy schemes of these nanostructures. Due to the analytical complexity of the effective nanostructure potential components for an electron, a rough approximation is often used, in which only the contribution from the internal electric field is stored [3] or grid numerical methods are used [7]. The method, which deals with the analytical calculation of the effective potential components and their sequential self-consistent approximation by solutions of the Schrödinger and Poisson equations, is effective enough [8].

Recently, for nitride resonant tunneling nanostructures (RTS), the spectra of acoustic phonons [9] have been investigated and the interaction of electrons with them [10] have been studied for the first time. The results obtained demonstrate significant differences in the spectra of acoustic phonons for multilayer nanostructures in comparison with

the results obtained on the basis of the single-well nanostructures simplified models [11].

An interesting case of processes in nitride nanosystems is that the piezoelectric effect arising, which is caused by the shear acoustic phonons in AlN/GaN plane nanostructures [12, 13]. As a result, the polarization effects in the nitride layers are revealed being more sufficient than these for arsenide semiconductors. The resulting piezoelectric effect is likely to have a significant effect on the spectrum of acoustic phonons and the spectral characteristics of electrons in such nanostructures. In fact, there are only two papers [12, 13] in which the spectrum of acoustic phonons was calculated from the multilayer Fibonacci nanostructure transparency coefficient in a certain frequency range of the electromagnetic field. Since the authors of these papers set somewhat different goals, in fact, the dependences of the acoustic phonons spectrum were only partially investigated, saying nothing about the electron-phonon interaction. Besides, the study of the transparency coefficient corresponds to the case, when the investigated nanostructure is placed into a medium in which waves can propagate freely. In such a model the nanostructure cannot be treated as a constituent part of a separate cascade, for example, because the condition for the components of elastic displacement and stress tensors going to zero will not be satisfied.

The proposed paper is structured as follows. In the first part, the theory of acoustic phonons and piezoelectric potential arising in layers of piezoelectric AlN/GaN nanostructure is developed on the basis of the elastic continuum model. In the second part, the theory of the stationary spectrum and wave functions of electrons in the approximated effective potential of the nanostructure is developed. This section also presents a developed consistent theory of the interaction of electrons with acoustic phonons due to the piezoelectric potential for arbitrary temperatures using the temperature Green's functions and the Dyson equation, based on solutions of the system of stationary Schrödinger and Poisson equations. The last section is devoted to calculations and investigation of the electronic and phonon spectra dependences. The dependences of the electronic spectrum levels temperature shifts and their decay rates due to the interaction with acoustic phonons are investigated.

2. Theory of the acoustic phonons spectrum and piezoelectric potential in the multilayer AlN/GaN nanostructure

The investigated nanostructure will be considered in the Cartesian coordinate system, the z axis being perpendicular to the interfaces between its layers (Fig. 1). Due to the need to ensure the arbitrariness of the choice of this nanostructure as a separate element of the nanodevice cascade, we will consider it to be placed in an external unstressed medium AlN corresponding to potential barriers. Accordingly, the potential wells of the nanostructure correspond to the GaN semiconductor medium.

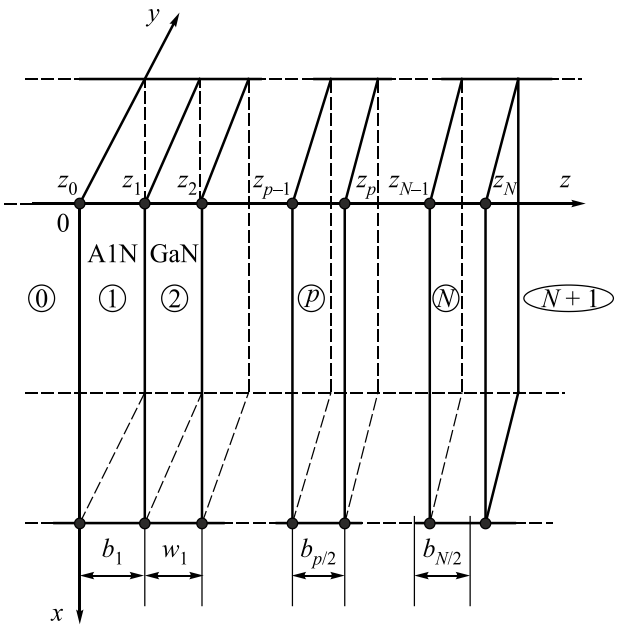

Fig. 1. Geometric scheme of the multilayer nanostructure of plane symmetry.

Taking into account various types of semiconductors forming the nanostructure, its density ρ, elastic constant tensor components C_{iklm}, piezoelectric constants e_{ikl} and dielectric constants ε_{ik} are dependent on the z coordinate:

$$\Phi(z) = \Phi^{(0)}(z)\theta(-z) + \sum_{p=1}^{N} \Phi^{(p)}(z)\left[\theta(z-z_{p-1}) - \theta(z-z_p)\right] + \Phi^{(N+1)}(z)\theta(z-z_N),$$

$$\Phi = \{\rho,\, C_{iklm},\, e_{ikl},\, \varepsilon_{ik}\}. \tag{1}$$

The components of elastic displacement for each of the layers of the studied nanostructure are obtained by solving the equation

$$\rho(z)\frac{\partial^2 u_i(\bar{r},t)}{\partial t^2} = \frac{\partial \sigma_{ik}(\bar{r},t)}{\partial x_k},$$

$$u_i(\bar{r},t) = u_i(x,y,z,t) = \begin{pmatrix} u_{i1} & u_{i2} & u_{i3} \end{pmatrix}^T, \tag{2}$$

where in (1) and (2): $i,k,l,m = (1;2;3)$, $x_1 = x$, $x_2 = y$; $x_3 = z$ according to the selected coordinate system.

The components of the stress tensor in the presence of the piezoelectric effect are conveniently represented as follows:

$$\sigma_{ik}(\bar{r},t) = C_{iklm}(z)u_{lm}(\bar{r},t) - e_{ikl}(z)E_l(\bar{r},t), \tag{3}$$

where the components of the strain tensor are as follows:

$$u_{lm}(\bar{r},t) = \frac{1}{2}\left(\frac{\partial u_l(\bar{r},t)}{\partial x_m} + \frac{\partial u_m(\bar{r},t)}{\partial x_l}\right). \tag{4}$$

Equation (3) being substituted into (2) taking into account (5), gives the equation of the second order:

$$\rho(z)\frac{\partial^2 u_i(\bar{r},t)}{\partial t^2}=\frac{\partial}{\partial x_k}\left(C_{iklm}(z)\frac{\partial u_l(\bar{r},t)}{\partial x_m}+e_{ikl}(z)\frac{\partial\phi(\bar{r},t)}{\partial x_l}\right), \tag{5}$$

since the electric field $E_l(\bar{r})$ belongs to the potential as $E_l(\bar{r},t)=-\partial\phi(\bar{r},t)/\partial x_l$.

The electric displacement vector is defined as follows:

$$\begin{aligned}D_i(\bar{r},t)&=e_{ikl}(z)u_{kl}(\bar{r},t)+\varepsilon_{ik}(\omega,z)E_k(\bar{r},t)=\\&=e_{ikl}(z)u_{kl}(\bar{r},t)-\varepsilon_{ik}(\omega,z)\frac{\partial\phi(\bar{r},t)}{\partial x_k},\end{aligned} \tag{6}$$

where the components of the permittivity tensor, which, as it is known [13, 14], form the matrix

$$\varepsilon_{ik}(\omega,z)=\begin{pmatrix}\varepsilon_{11}(\omega,z) & 0 & 0\\ 0 & \varepsilon_{11}(\omega,z) & 0\\ 0 & 0 & \varepsilon_{33}(\omega,z)\end{pmatrix}, \tag{7}$$

where for binary semiconductors, depending on the frequency, we have

$$\begin{aligned}\varepsilon_{11}(\omega,z)&=\varepsilon_\infty(z)\frac{\omega^2-\omega^2_{LO(E_1)}(z)}{\omega^2-\omega^2_{TO(E_1)}(z)},\\ \varepsilon_{33}(\omega,z)&=\varepsilon_\infty(z)\frac{\omega^2-\omega^2_{LO(A_1)}(z)}{\omega^2-\omega^2_{TO(A_1)}(z)},\end{aligned} \tag{8}$$

where ε_∞ is high-frequency dielectric permittivity, ω_{LO} and ω_{TO} are the frequencies of longitudinal and transverse optical phonons, respectively defined in the vicinity of the Γ-point as irreducible representations $A_1(z)$ and $E_1(xy)$.

Further, having assumed, that there are no free charges in the nanostructure, we get

$$\mathrm{div}D=\frac{\partial D}{\partial x_k}=0, \tag{9}$$

which results in

$$\frac{\partial}{\partial x_l}\left(e_{ikl}(z)\frac{\partial u_k(\bar{r},t)}{\partial x_i}\right)-\frac{\partial}{\partial x_i}\left(\varepsilon_{ik}(\omega,z)\frac{\partial\phi(\bar{r},t)}{\partial x_k}\right)=0. \tag{10}$$

Having presented the Eqs. (5) and (10) for an arbitrarily chosen *p*th layer of the nanosystem, we have a system of coupled differential equations:

$$\begin{cases}\rho^{(p)}\dfrac{\partial^2 u_i(\bar{r},t)}{\partial t^2}-C^{(p)}_{iklm}\dfrac{\partial^2 u_l(\bar{r},t)}{\partial x_k\partial x_m}-e^{(p)}_{ikl}\dfrac{\partial^2\phi(\bar{r},t)}{\partial x_k\partial x_l}=0,\\ e^{(p)}_{ikl}\dfrac{\partial^2 u_k(\bar{r},t)}{\partial x_i\partial x_l}-\varepsilon^{(p)}_{ik}(\omega)\dfrac{\partial^2\phi(\bar{r},t)}{\partial x_i\partial x_k}=0.\end{cases} \tag{11}$$

It is convenient to solve the system of equations (11) at first by passing to Voigt's notation: $C^{(p)}_{iklm}\to C^{(p)}_{sn}$; $e^{(p)}_{ikl}\to e^{(p)}_{sn}$. Taking into account the symmetry of the problem, it is assumed that the deformation of the nanostructure in the plane *xOy* and along the axis *Oz* is isotropic [9, 11–13], then the piezoelectric effect is completely described by the displacement $(0,u_2(\bar{r}),0)=(0,u_2(x,z),0)$ and potential $\phi(\bar{r})=\phi(x,z)$. Taking into account the form of tensors $C^{(p)}_{sn}$, $e^{(p)}_{sn}$ for crystals with a wurtzite-type lattice [15], from system (11), we obtain the equations for u_2 and ϕ:

$$\begin{cases}\rho^{(p)}\dfrac{\partial^2 u_2(x,z,t)}{\partial t^2}-C^{(p)}_{44}\left(\dfrac{\partial^2 u_2(x,z,t)}{\partial x^2}+\dfrac{\partial^2 u_2(x,z,t)}{\partial z^2}\right)-e^{(p)}_{15}\left(\dfrac{\partial^2\phi(x,z,t)}{\partial x^2}+\dfrac{\partial^2\phi(x,z,t)}{\partial z^2}\right)=0,\\ e^{(p)}_{15}\left(\dfrac{\partial^2 u_2(x,z,t)}{\partial x^2}+\dfrac{\partial^2 u_2(x,z,t)}{\partial z^2}\right)-\varepsilon^{(p)}_{11}(\omega)\dfrac{\partial^2\phi(x,z,t)}{\partial x^2}-\varepsilon^{(p)}_{33}(\omega)\dfrac{\partial^2\phi(x,z,t)}{\partial z^2}=0.\end{cases} \tag{12}$$

Solutions for system (12) are found by the method described below. The time dependence of the displacement can be considered harmonious, that is: $u_2(x,z,t)=u_2(x,z)e^{-i\omega t}$ and $\phi(x,z,t)=\phi(x,z)e^{-i\omega t}$. Than we represent the desired solution in the form of a column matrix:

$$U(x,z)=\begin{pmatrix}u_2(x,z)\\ \phi(x,z)\end{pmatrix}=U(z)e^{iqx}=\begin{pmatrix}u_2(z)\\ \phi(z)\end{pmatrix}e^{iqx}, \tag{13}$$

which after substitution in (12) looks like:

$$\begin{cases}-C^{(p)}_{44}\dfrac{d^2u_2(z)}{dz^2}+(q^2C^{(p)}_{44}-\rho^{(p)}\omega^2)u_2(z)+q^2e^{(p)}_{15}\phi(z)-e^{(p)}_{15}\dfrac{d^2\phi(z)}{dz^2}=0,\\ e^{(p)}_{15}\dfrac{d^2u_2(z)}{dz^2}-q^2e^{(p)}_{15}u_2(z)+q^2\varepsilon^{(p)}_{11}(\omega)\phi(z)-\varepsilon^{(p)}_{33}(\omega)\dfrac{d^2\phi(z)}{dz^2}=0.\end{cases} \tag{14}$$

From the first Eq. (14) it is seen that the acoustic phonons caused by the displacement $u_2(z)$, have the same nature as the shear acoustic phonons (SH). Besides, this equation at $\phi(z)\to 0$, looks like the equation for these phonons obtained in the paper [9].

Than the following notation is introduced:

$$a^{(p)} = -C_{44}^{(p)},$$
$$b^{(p)} = b^{(p)}(q,\omega) = q^2 C_{44}^{(p)} - \rho^{(p)}\omega^2,$$
$$c^{(p)} = c^{(p)}(q) = q^2 e_{15}^{(p)},$$
$$d^{(p)} = -e_{15}^{(p)}, \qquad (15)$$
$$e^{(p)} = e^{(p)}(q,\omega) = q^2 \varepsilon_{11}^{(p)}(\omega),$$
$$f^{(p)} = f^{(p)}(\omega) = -\varepsilon_{33}^{(p)}(\omega).$$

Then system (14) turns out to be equivalent to such equation:

$$A^{(p)} \frac{d^2 U^{(p)}(z)}{dz^2} - B^{(p)} U^{(p)}(z) = 0, \qquad (16)$$

where

$$A^{(p)} = \begin{pmatrix} a^{(p)} & d^{(p)} \\ -d^{(p)} & f^{(p)} \end{pmatrix}; \; B^{(p)} = \begin{pmatrix} -b^{(p)} & -c^{(p)} \\ c^{(p)} & -e^{(p)} \end{pmatrix}. \qquad (17)$$

Solutions of the Eq. (16) are expected to look like:

$$U^{(p)}(z) = \mu^{(p)} e^{\lambda z}; \; \mu^{(p)} = \begin{pmatrix} \mu_1^{(p)} \\ \mu_2^{(p)} \end{pmatrix}. \qquad (18)$$

In results in the equation for finding the eigenvalues λ and functions $\mu^{(p)}$:

$$\left(A^{(p)}\lambda^2 - B^{(p)}\right)\mu^{(p)} = 0. \qquad (19)$$

The equation for finding the eigenvalues results in the biquadratic equation for λ:

$$\lambda^4 + \frac{2c^{(p)}d^{(p)} + a^{(p)}e^{(p)} + b^{(p)}f^{(p)}}{\left(d^{(p)}\right)^2 + a^{(p)}f^{(p)}}\lambda^2 + \frac{\left(c^{(p)}\right)^2 + b^{(p)}e^{(p)}}{\left(d^{(p)}\right)^2 + a^{(p)}f^{(p)}} = 0. \qquad (20)$$

Taking into account (15), these solutions are as follows:

$$\lambda_{1,2,3,4} = \pm\sqrt{-\frac{2c^{(p)}d^{(p)} + a^{(p)}e^{(p)} + b^{(p)}f^{(p)}}{2\left\{\left(d^{(p)}\right)^2 + a^{(p)}f^{(p)}\right\}} \pm \sqrt{\left[\frac{2c^{(p)}d^{(p)} + a^{(p)}e^{(p)} + b^{(p)}f^{(p)}}{2\left\{\left(d^{(p)}\right)^2 + a^{(p)}f^{(p)}\right\}}\right]^2 - \frac{\left(c^{(p)}\right)^2 + b^{(p)}e^{(p)}}{\left(d^{(p)}\right)^2 + a^{(p)}f^{(p)}}}} =$$
$$= \pm\left\{\frac{2\left(qe_{15}^{(p)}\right)^2 + C_{44}^{(p)}q^2\varepsilon_{11}^{(p)}(\omega) - (q^2C_{44}^{(p)} - \rho^{(p)}\omega^2)\varepsilon_{33}^{(p)}(\omega)}{2\left\{\left(e_{15}^{(p)}\right)^2 + \varepsilon_{33}^{(p)}(\omega)C_{44}^{(p)}\right\}} \pm \right. \qquad (21)$$
$$\left. \pm\left\{\left[\frac{2\left(qe_{15}^{(p)}\right)^2 + C_{44}^{(p)}q^2\varepsilon_{11}^{(p)}(\omega) + (q^2C_{44}^{(p)} - \rho^{(p)}\omega^2)\varepsilon_{33}^{(p)}(\omega)}{2\left\{\left(e_{15}^{(p)}\right)^2 + \varepsilon_{33}^{(p)}(\omega)C_{44}^{(p)}\right\}}\right]^2 - \frac{\left(q^2e_{15}^{(p)}\right)^2 + (q^2C_{44}^{(p)} - \rho^{(p)}\omega^2)q^2\varepsilon_{11}^{(p)}(\omega)}{\left(e_{15}^{(p)}\right)^2 + \varepsilon_{33}^{(p)}(\omega)C_{44}^{(p)}}\right\}^{\frac{1}{2}}\right\}^{\frac{1}{2}},$$

$$\lambda_1 = -\lambda_2; \; \lambda_3 = -\lambda_4.$$

where the index "*p*" is omitted for convenience.

The eigenfunctions $\mu^{(p)}$ are found from Eq. (19) by the Cayley–Hamilton theorem:

$$\begin{pmatrix} a^{(p)}\lambda_n^2 + b^{(p)} & d^{(p)}\lambda_n^2 + c^{(p)} \\ -d^{(p)}\lambda_n^2 - c^{(p)} & f^{(p)}\lambda_n^2 + e^{(p)} \end{pmatrix}\begin{pmatrix} a_{1,n}^{(p)} \\ a_{2,n}^{(p)} \end{pmatrix} = 0; \; n = 1-4, \qquad (22)$$

from which we have

$$a_{1,n}^{(p)} = d^{(p)}\lambda_n^2 + c^{(p)} = e_{15}^{(p)}(q^2 - \lambda_n^2), \; a_{2,n}^{(p)} =$$
$$= -(a^{(p)}\lambda_n^2 + b^{(p)}) = C_{44}^{(p)}\lambda_n^2 - q^2C_{44}^{(p)} + \rho^{(p)}\omega^2. \qquad (23)$$

Thus, the final solutions of the system (14) are:

$$u_2^{(p)}(z) = \left\|V_1^{(p)}\right\| a_{1,1}^{(p)}A_1^{(p)}e^{\lambda_1 z} + \left\|V_2^{(p)}\right\| a_{1,2}^{(p)}B_1^{(p)}e^{\lambda_2 z} + \left\|V_3^{(p)}\right\| a_{1,3}^{(p)}C_1^{(p)}e^{\lambda_3 z} + \left\|V_4^{(p)}\right\| a_{1,4}^{(p)}D_1^{(p)}e^{\lambda_4 z} =$$
$$= e_{15}^{(p)}\left(\left\|V_1^{(p)}\right\|(q^2 - \lambda_1^2)\left(A_1^{(p)}e^{\lambda_1 z} + B_1^{(p)}e^{-\lambda_1 z}\right) + \left\|V_2^{(p)}\right\|(q^2 - \lambda_2^2)\left(C_1^{(p)}e^{\lambda_2 z} + D_1^{(p)}\lambda_2 e^{-\lambda_2 z}\right)\right),$$
$$\phi^{(p)}(z) = \left\|V_1^{(p)}\right\| a_{2,1}^{(p)}A_1^{(p)}e^{\lambda_1 z} + \left\|V_2^{(p)}\right\| a_{2,2}^{(p)}B_1^{(p)}e^{\lambda_2 z} + \left\|V_3^{(p)}\right\| a_{2,3}^{(p)}C_1^{(p)}e^{\lambda_3 z} + \left\|V_4^{(p)}\right\| a_{2,4}^{(p)}D_1^{(p)}e^{\lambda_4 z} = \qquad (24)$$
$$= \left\|V_1^{(p)}\right\|\left(C_{44}^{(p)}\lambda_1^2 - q^2C_{44}^{(p)} + \rho^{(p)}\omega^2\right)\left(A_1^{(p)}e^{\lambda_1 z} + B_1^{(p)}e^{-\lambda_1 z}\right) +$$
$$+ \left\|V_2^{(p)}\right\|\left(C_{44}^{(p)}\lambda_2^2 - q^2C_{44}^{(p)} + \rho^{(p)}\omega^2\right)\left(C_1^{(p)}e^{\lambda_2 z} + D_1^{(p)}e^{-\lambda_2 z}\right),$$

where

$$\left\|V_n^{(p)}\right\| = 1\Big/\sqrt{\left|a_{1,n}^{(p)}\right|^2 + \left|a_{2,n}^{(p)}\right|^2} =$$

$$= \left\{\left|e_{15}^{(p)}(q^2-\lambda_n^2)\right|^2 + \left|C_{44}^{(p)}\lambda_n^2 - q^2C_{44}^{(p)} + \rho^{(p)}\omega^2\right|^2\right\}^{-1/2}. \tag{25}$$

In the external environment, the elastic displacement and potential should follow to zero, that is

$$\lim_{z\to\pm\infty}\begin{pmatrix} u_2(z) \\ \phi(z)\end{pmatrix} = 0, \tag{26}$$

from where $A_1^{(0)} = C_1^{(0)} = B_1^{(N+1)} = D_1^{(N+1)} = 0$.

To determine all unknown coefficients, we use the boundary conditions at the boundaries of all layers of the nanostructure, which are fulfilled for elastic displacement $u_2^{(p)}(z)e^{i(qx-\omega t)}$, for potential $\phi^{(p)}(z)e^{i(qx-\omega t)}$, for component $\sigma_{zy}^{(p)}(z) = \sigma_{32}^{(p)}(z)$ of the stress tensor, defined as follows:

Fraction $\frac{1}{2}$ before $C_{44}^{(p)}$ must be, that is:

$$\sigma_{32}^{(p)}(z) = \frac{1}{2}C_{44}^{(p)}\left(\frac{\partial u_z^{(p)}(x,z)}{\partial y} + \frac{\partial u_y^{(p)}(x,z)}{\partial z}\right) + e_{15}^{(p)}E_2^{(p)}(\omega,x,z) =$$

$$= \frac{1}{2}C_{44}^{(p)}\frac{du_2^{(p)}(z)}{dz}e^{i(\omega t-qx)} + e_{15}^{(p)}\frac{\partial\left(\phi^{(p)}(z)e^{i(qx-\omega t)}\right)}{\partial y} = \tag{27}$$

$$= \frac{1}{2}e_{15}^{(p)}C_{44}^{(p)}\left(\left\|V_1^{(p)}\right\|(q^2-\lambda_1^2)\lambda_1\left(A_1^{(p)}e^{\lambda_1 z} - B_1^{(p)}e^{-\lambda_1 z}\right) + \left\|V_2^{(p)}\right\|(q^2-\lambda_2^2)\lambda_2\left(C_1^{(p)}e^{\lambda_2 z} - D_1^{(p)}\lambda_2 e^{-\lambda_2 z}\right)\right),$$

and from the normal component of the electric displacement vector as well:

$$D_3^{(p)}(z) = e_{31}^{(p)}\frac{\partial\left(u_2^{(p)}(z)e^{i(qx-\omega t)}\right)}{\partial y} + \varepsilon_{33}^{(p)}(\omega)\frac{\partial\left(\phi^{(p)}(z)e^{i(qx-\omega t)}\right)}{\partial z} =$$

$$= \varepsilon_{33}^{(p)}(\omega)\left\{\left\|V_1^{(p)}\right\|\lambda_1\left(C_{44}^{(p)}\lambda_1^2 - q^2C_{44}^{(p)} + \rho^{(p)}\omega^2\right)\left(A_1^{(p)}e^{\lambda_1 z} - B_1^{(p)}e^{-\lambda_1 z}\right) + \right. \tag{28}$$

$$\left. + \left\|V_2^{(p)}\right\|\lambda_2\left(C_{44}^{(p)}\lambda_2^2 - q^2C_{44}^{(p)} + \rho^{(p)}\omega^2\right)\left(B_1^{(p)}e^{\lambda_2 z} + D_1^{(p)}e^{-\lambda_2 z}\right)\right\}e^{i(qx-\omega t)}.$$

These boundary conditions are:

$$\begin{cases} u_2^{(p)}(z)\Big|_{z\to z_p-0} = u_2^{(p+1)}(z)\Big|_{z\to z_p+0}, \\ \phi^{(p)}(z)\Big|_{z\to z_p-0} = \phi^{(p+1)}(z)\Big|_{z\to z_p+0}, \\ \sigma_{32}^{(p)}(z)\Big|_{z\to z_p-0} = \sigma_{32}^{(p+1)}(z)\Big|_{z\to z_p+0}, \\ D_3^{(p)}(z)\Big|_{z\to z_p-0} = D_3^{(p+1)}(z)\Big|_{z\to z_p+0}. \end{cases} \tag{29}$$

Let us introduce such ket vectors:

$$\left|f^{(p)}\right\rangle = \left(A_1^{(p)} \quad B_1^{(p)} \quad C_1^{(p)} \quad D_1^{(p)}\right)^T, \tag{30}$$

then, according to the transfer matrix method, we obtain:

$$\left|f^{(0)}\right\rangle = \prod_{p=0}^{N} T^{(p,p+1)}(q,\omega)\left|f^{(N+1)}\right\rangle,\ T^{(p,p+1)}(q,\omega) = \left(t^{(p)}(q,\omega)\right)^{-1}t^{(p+1)}(q,\omega),$$

$$t^{(p)}(q,\omega) = \begin{pmatrix} \alpha_1^{(p)}(q,\omega) & \alpha_1^{(p)}(q,\omega) & \alpha_2^{(p)}(q,\omega) & \alpha_2^{(p)}(q,\omega) \\ \beta_1^{(p)}(q,\omega) & \beta_1^{(p)}(q,\omega) & \beta_2^{(p)}(q,\omega) & \beta_2^{(p)}(q,\omega) \\ \gamma_1^{(p)}(q,\omega) & -\gamma_1^{(p)}(q,\omega) & \gamma_2^{(p)}(q,\omega) & -\gamma_2^{(p)}(q,\omega) \\ \delta_1^{(p)}(q,\omega) & -\delta_1^{(p)}(q,\omega) & \delta_2^{(p)}(q,\omega) & -\delta_2^{(p)}(q,\omega) \end{pmatrix}\begin{pmatrix} e^{\lambda_1 z^{(p)}} \\ e^{-\lambda_1 z^{(p)}} \\ e^{\lambda_2 z^{(p)}} \\ e^{-\lambda_2 z^{(p)}} \end{pmatrix},$$

$$\alpha_1^{(p)}(q,\omega) = e_{15}^{(p)}\left\|V_1^{(p)}\right\|(q^2-\lambda_1^2),\ \alpha_2^{(p)}(q,\omega) = e_{15}^{(p)}\left\|V_2^{(p)}\right\|(q^2-\lambda_2^2),$$

$$\beta_1^{(p)}(q,\omega) = \left\|V_1^{(p)}\right\|\left(C_{44}^{(p)}\lambda_1^2 - q^2C_{44}^{(p)} + \rho^{(p)}\omega^2\right),\ \beta_2^{(p)}(q,\omega) = \left\|V_2^{(p)}\right\|\left(C_{44}^{(p)}\lambda_2^2 - q^2C_{44}^{(p)} + \rho^{(p)}\omega^2\right), \tag{31}$$

$$\gamma_1^{(p)}(q,\omega) = e_{15}^{(p)}C_{44}^{(p)}\left\|V_1^{(p)}\right\|(q^2-\lambda_1^2)\lambda_1,\ \gamma_2^{(p)}(q,\omega) = e_{15}^{(p)}C_{44}^{(p)}\left\|V_2^{(p)}\right\|(q^2-\lambda_2^2)\lambda_2,$$

$$\delta_1^{(p)}(q,\omega) = \varepsilon_{33}^{(p)}(\omega)\left\|V_1^{(p)}\right\|\lambda_1\left(C_{44}^{(p)}\lambda_1^2 - q^2C_{44}^{(p)} + \rho^{(p)}\omega^2\right),$$

$$\delta_2^{(p)}(q,\omega) = \varepsilon_{33}^{(p)}(\omega)\left\|V_2^{(p)}\right\|\lambda_2\left(C_{44}^{(p)}\lambda_2^2 - q^2C_{44}^{(p)} + \rho^{(p)}\omega^2\right).$$

The spectrum of acoustic phonons $\omega_{n_1} = \omega(q_{n_1})$ is now determined from the dispersion equation:

$$\det\left\{\prod_{p=0}^{N} T^{(p,p+1)}(q,\omega)\right\} = 0. \qquad (32)$$

Using boundary conditions (29), we express the coefficients $A_1^{(p)}$, $B_1^{(p)}$, $C_1^{(p)}$, $D_1^{(p)}$ in terms of one of them. This coefficient is obtained from the normalization condition for the displacement values u_2, which is

$$\int_{-\infty}^{+\infty} \rho(z) u_2^*(q,\omega_q,z) u_2(q',\omega_{q'},z)dz = \frac{\hbar}{2\Delta l_x \Delta l_y \omega}\delta_{qq'}, \qquad (33)$$

where $\Delta l_x \Delta l_y$ is the cross-sectional area of the nanostructure with the *xOy* plane, moreover, Δl_x, $\Delta l_y >> z_N$.

Having performed a Fourier series $u_2(q,\omega_q,z)$ for the displacement and potential $\phi(q,\omega_q,z)$:

$$\begin{pmatrix} u_2(q,\omega_{n_1q},r) \\ \phi(q,\omega_q,z) \end{pmatrix} = \sum_{n_1q} \begin{pmatrix} u_2(q,\omega_{n_1q},z) \\ \phi(q,\omega_{n_1q},z) \end{pmatrix} e^{i\overline{qr}}, \qquad (34)$$

where the functions $u_2(q,\omega_{n_1q},z)$ and $\phi(q,\omega_{n_1q},z)$, which play the role of expansion coefficients, containing all possible modes of acoustic phonons ω_{n_1q}.

Now passing from the Fourier components to the generalized coordinates and momentum, and then to the operators of occupation numbers according to [14], we obtain the elastic displacement operator in the representation of occupation numbers:

$$\hat{u}_2(q,\omega_{n_1q},r) = \sum_{p=0}^{N}\sum_{n_1q}\sqrt{\frac{\hbar}{2\Delta l_x \Delta l_y \rho^{(p)}\omega_{n_1q}}}\left(\hat{b}_{n_1}(-q)+\hat{b}_{n_1}(q)\right)\hat{w}_2^{(p)}(q,\omega_{n_1q},z)e^{i\overline{qr}}\left[\theta(z-z_{p-1})-\theta(z-z_p)\right],$$
$$\hat{w}_2^{(p)}(q,\omega_{n_1q},z) = \sqrt{\rho^{(p)}}\hat{u}_2^{(p)}(q,\omega_{n_1q},z),\ z_1 = -\infty. \qquad (35)$$

To determine $\phi(q,\omega_{n_1q},z)$, we substitute expansion (34), taking into account (35), into the second equation of system (14). After simplifications we obtain the differential equation:

$$\varepsilon_{33}^{(p)}(\omega)\frac{d^2\phi^{(p)}(q,\omega_{n_1q},z)}{dz^2} - q^2\varepsilon_{11}^{(p)}(\omega)\phi^{(p)}(q,\omega_{n_1q},z) =$$
$$= e_{15}^{(p)}\sqrt{\frac{\hbar}{2\Delta l_x \Delta l_y \rho^{(p)}\omega_{n_1q}}}\left[\frac{d^2\hat{w}_2^{(p)}(q,\omega_{n_1q},z)}{dz^2} - q^2\hat{w}_2^{(p)}(q,\omega_{n_1q},z)\right], \qquad (36)$$

its solution is not presented due to its very cumbersome nature.

Now, the Hamiltonian of acoustic phonons in the second quantization representation looks like:

$$\hat{H}_{ac} = \sum_{n_1q}\hbar\omega_{n_1q}\left(\hat{b}_{n_1q}^{+}\hat{b}_{n_1q} + \frac{1}{2}\right), \qquad (37)$$

where $\hat{b}_{n_1q}^{+}$ and $\hat{b}_{n_1q}$ are the bosonic creation and annihilation operators of the phonon state respectively.

3. Spectrum and wave functions of an electron in the nanostructure effective potential. Renormalization of the electron spectrum by interaction with acoustic phonons

The energy scheme of the investigated AlN/GaN nanostructure substantially depends on the internal electric field created in its layers by the total polarization $P^{(\text{total})} = P_{Pz} + P_{Sp}$, where P_{Pz} is the piezoelectric polarization, P_{Sp} is the spontaneous polarization [6]. Besides, due to different polarization values surface charges with a density $\sigma^{(p)} = P_{p+1} - P_p$ appear at the heterointerfaces of the nanostructure.

The interaction of an electron with an internal electric field is defined as follows:

$$V_E(z) = e\sum_{p=1}^{N}(-1)^{p-1}(F_p z - F_{p-1}z_{p-1})\left[\theta(z-z_{p-1})-\theta(z-z_p)\right], \qquad (38)$$

where the electric field strength in an arbitrary layer of the nanostructure is obtained from the condition, when the total value of the voltage applied to the nanostructure is zero [3, 7, 8]:

$$F_0 = 0;$$
$$F_p = \sum_{\substack{k=1 \\ k\neq p}}^{N}\left(P_k - P_p\right)(z_k - z_{k+1})/\varepsilon_\infty^{(k)} \Big/ \varepsilon_\infty^{(p)}\sum_{k=1}^{N}(z_k - z_{k+1})/\varepsilon_\infty^{(k)}. \qquad (39)$$

In addition, there is the so-called exchange correlation potential in the Hedin–Lundqvist approximation [7, 8, 15]:

$$V_{HL}(z) = -\frac{1}{4\pi}\left(\frac{9}{4\pi^2}\right)^{1/3} \times$$
$$\times\left[1+\frac{0,6213 r_s}{21}\ln\left(1+\frac{21}{r_s(z)}\right)\right]\frac{e^2}{\varepsilon_0 r_s(z)\varepsilon_\infty(z)a_B^*(z)},$$
$$r_s(z) = \left(4\pi a_B^{*3} n(z)/3\right)^{-1/3},\ a_B^*(z) = \varepsilon_\infty(z)/m(z)a_B, \qquad (40)$$

where a_B is the Bohr radius.

Without taking into account the influence of the internal electric field and fields caused by the distribution of static charge in nanostructures, choosing zero energy for the bottom of the conduction band, for potential barriers, we have

$$\Delta E_C(z) = 0.765(E_g(\mathrm{AlN}) - E_g(\mathrm{GaN})). \qquad (41)$$

The temperature dependence of the bandgap is calculated using the Varshni ratio:

$$E_g(T) = E_g(0) - \frac{\alpha T^2}{\beta + T}, \qquad (42)$$

where $E_g(0) = E_g^{\mathrm{AlN}}(0) =$ is band gap at $T = 0\,\mathrm{K}$, α, β are the Varshni parameters [8, 15].

For functioning of nanodevices, the main role is played by the movement of electrons along the *Oz* axis. For such a motion, the levels of states of the electronic spectrum E_n and the corresponding wave functions $\Psi_E(z)$ are solutions of the system of stationary Schrödinger and Poisson equations:

$$\begin{cases} -\frac{\hbar^2}{2}\frac{d}{dz}\left(\frac{1}{m(z)}\frac{d\Psi(z)}{dz}\right) + V(z)\Psi_E(z) = E\Psi_E(z), \\ \frac{d}{dz}\left(\varepsilon_\infty(z)\frac{dV_H(z)}{dz}\right) = -\frac{e}{\varepsilon_0}\rho^{(\mathrm{elect})}(z), \end{cases} \qquad (43)$$

where the charge density in the nanostructure is defined as follows:

$$\rho^{(\mathrm{elect})}(z) = e(N_D^+ - n(z)) + \sum_{p=1}^{N}\sigma_p\delta(z - z_p), \qquad (44)$$

where N_D^+ is the concentration of ionized donor impurities,

$$n(z) = \frac{m(z)k_BT}{\pi\hbar^2}\sum_n \left|\Psi(E_n, z)\right|^2 \ln\left|1 + \exp\left(\frac{E_F - E_n}{k_BT}\right)\right|$$

is the concentration of electrons creating a static charge inside a nanostructure, E_F is the Fermi level for the nanostructure [7, 8, 16].

In total, the quantities given by Eqs. (38), (40), and (41) constitute the nanostructure effective potential for an electron:

$$V(z) = \Delta E_C(z) + V_E(z) + V_{HL}(z) + V_H(z). \qquad (45)$$

The last term $V_H(z)$, which is the solution of the Poisson equation, specifies the interaction of an electron with the total charge inside the nanostructure (43).

The solution of system (43) cannot be found exactly. It is usually found numerically [7]. However, in our case, we can use the analytical method [8] calculating the components (44) using the solutions of system (43) found with the required accuracy, where:

$$V_H(z) = \sum_{p=1}^{N} V_H^{(p)}(z)\left[\theta(z - z_{p-1}) - \theta(z - z_p)\right];$$
$$V_H^{(p)}(z) = -\frac{e}{\varepsilon_0\varepsilon_\infty^{(p)}}\int_0^z\left\{\int_0^z\left[e\left(N_D^+ - \frac{m_{(p)}k_BT}{\pi\hbar^2}\sum_n\left|\Psi(E_n, z)\right|^2\ln\left|1 + \exp\left(\frac{E_F - E_n}{k_BT}\right)\right|\right) + \sigma_p\delta(z - z_p)\right]dz\right\}dz. \qquad (46)$$

Thus, the wave function in the approximated potential

$$U_{\mathrm{appr}}(z) = \sum_{p=1}^{N}\sum_{l=0}^{M}\frac{V(z_{p_{l+1}}) - V(z_{p_l})}{z_{p_{l+1}} - z_{p_l}} z\left[\theta(z - z_{p_l}) - \theta(z - z_{p_{l+1}})\right] \qquad (47)$$

can be presented in the external environment as an exponent decreasing at $z \pm \infty$, and inside the nanostructure as a linear combination of the Airy functions $Ai(z)$, $Bi(z)$:

$$\Psi(E, z) = A^{(0)}e^{\chi^{(0)}z}\theta(-z) + \sum_{p=1}^{N}\sum_{l=0}^{M}\left\{A^{(p_l)}Ai\left[\zeta^{(p_l)}(z)\right] + B^{(p_l)}Bi\left[\zeta^{(p_l)}(z)\right]\right\}\left[\theta(z - z_{p_l}) - \theta(z - z_{p_{l+1}})\right] +$$
$$+ B^{(N+1)}e^{-\chi^{(0)}z}\theta(z - z_N),\ \zeta^{(p_l)}(z) = \left(2m^{(p_l)}eF(z_{p_l})/\hbar^2\right)^{1/3}\left[(\Delta E_C(z) - E)/eF(z_{p_l}) - z\right]. \qquad (48)$$

The double sums in relation (46) define a piecewise continuous function formed by the splitting points $z_{p_l} = l/2M(z_p - z_{p-1})$, $p = 1...N$, $z_0 = 0$ of an arbitrary *p*th layer of the nanostructure, M is the number of these splits.

The dispersion equation, from which the levels of the stationary electronic spectrum E_n are determined, is obtained by applying the continuity conditions for the wave function (46) and the flows of its probabilities at the boundaries z_{p_l} of each of the layers (it is clear that the set of points $\{z_{p_l}\}$ includes all the heterointerfaces of the nanostructure), with a thickness $z_{p_l+1} - z_{p_l}$:

$$\Psi^{(p_l)}(E, z_{p_l}) = \Psi^{(p_{l+1})}(E, z_{p_{l+1}});\ \left.\frac{d\Psi_n^{(p_l)}(E, z)}{m(z)dz}\right|_{z=z_{p_l}-0} = \left.\frac{d\Psi_n^{(p_{l+1})}(E, z)}{m(z)dz}\right|_{z=z_{p_l}+0}. \qquad (49)$$

In the general case, assuming, that the geometric dimensions of the cross-section of the nanostructure are much larger than it longitudinal dimensions, that is Δl_x, $\Delta l_y >> z_N$,

in this case, the wave function of the electron can be represented as a Bloch-like function [10, 17]:

$$\Psi_{E\bar{k}_0}(R) = \Psi_{E\bar{k}_0}(\bar{r}, z) = \frac{1}{\sqrt{\Delta l_x \Delta l_y}} e^{i\bar{k}\bar{r}} \Psi_E(z),\ R = (x, y, z), \tag{50}$$

where $\bar{r}$ is the vector in plane xOy, $\bar{k}$ is the electron quasimomentum. In this case, the total energy, describing the longitudinal and transverse motion of the electron, is as follows:

$$E_{n\bar{k}} = E_n + \frac{\hbar^2 k^2}{2m_n^{(\text{eff})}}, \tag{51}$$

where the effective mass averaged over all layers of the nanostructure is introduced, which is determined by the expression [17]:

$$\frac{1}{m_n^{(\text{eff})}} = \int_{-\infty}^{+\infty} \left(\left| \Psi_n(E_n, z) \right|^2 / m(z) \right) dz. \tag{52}$$

The electron wave function $\Psi_n(E_n, z)$ is normalized with the condition:

$$\int_{-\infty}^{+\infty} \Psi_n(E_n, z) \Psi_{n'}(E_{n'}, z) dz = \delta_{nn'}. \tag{53}$$

Next, having applied the boundary conditions one can determine the coefficients $A^{(0)}$, $B^{(6)}$, $A^{(p_l)}$, $B^{(p_l)}$ and thus fully determine the wave function $\Psi_n(E_n, z)$.

The transition from the coordinate image to the second quantization image is performed by introducing a quantized wave function:

$$\hat{\Psi}(R) = \sum_{n\bar{k}} \Psi_{n\bar{k}}(\bar{r}, z) \hat{a}_{n\bar{k}} = \sum_{\bar{k}} \sum_{n} \Psi_{n\bar{k}}(\bar{r}, z) \hat{a}_{n\bar{k}}. \tag{54}$$

In this case, the Hamiltonian of noninteracting electrons in the second quantization image will look like:

$$\hat{H}_e = \int \hat{\Psi}(R) \hat{H}_e(R) \hat{\Psi}^+(R) dR = \sum_{n,\bar{k}} E_{n\bar{k}} \hat{a}^+_{n\bar{k}} \hat{a}_{n\bar{k}}, \tag{55}$$

where the total energy $E_{n\bar{k}}$ is determined in accordance with the expression (51), where $\hat{a}^+_{n\bar{k}}$ and $\hat{a}_{n\bar{k}}$ are the fermionic operators of creation and annihilation of electronic states respectively.

The deformation potential due to the stress tensor components ε_{ij} and the deformation potential constants a_{1c}, a_{2c} is determined for a crystal lattice of the wurtzite type as $\Delta E^{\text{def}} = a_{1c}\varepsilon_{zz} + a_{1c}(\varepsilon_{xx} + \varepsilon_{yy}) = 0$ [18–20], since, as for the components $[0, u_2(x, z), 0]$, taking into account (35), it follows, that $\varepsilon_{yy} = 0$ and $\varepsilon_{xx} = \varepsilon_{zz} = 0$ from the problem statement. Thus, in the presence of the piezoelectric effect, electrons and shear acoustic phonons do not interact either due the deformation potential, as in the case without taking into account the piezoelectric effect. However, as can be seen further, such interaction is possible due to the piezoelectric potential. The Hamiltonian of this interaction is described by the expression:

$$\hat{H}^{pz} = \sum_{q n_1} \sum_{p=1}^{N} \phi^{(p)}(q, \omega_{n_1 q}, z)(b_{n_1}(q) + b^+_{n_1}(-q)) e^{i\bar{q}\bar{r}} \times \times \left[\theta(z - z_{p-1}) - \theta(z - z_{p+1}) \right]. \tag{56}$$

Then, the Hamiltonian describing the interaction of electrons with acoustic phonons due to the piezoelectric potential looks like:

$$\hat{H}_{e-pz} = \sum_{n,\, n',\, n_1,\, \bar{k},\, \bar{q}} F_{nn_1}(q) \hat{a}^+_{n',\, \bar{k}+\bar{q}} \hat{a}_{n\bar{k}} \left[b_{n_1}(q) + b^+_{n_1}(-q) \right], \tag{57}$$

where the binding function is

$$F_{nn_1n'}(q) = \int_{z_{p-1}}^{z_p} \Psi^{(p)}(E_n, z) \phi^{(p)}(q, \omega_{n_1 q}, z) e^{i\bar{q}\bar{r}} \Psi^{*(p)}_{n'}(E_n, z) dz. \tag{58}$$

Thus, the Hamiltonian of the electron-acoustic phonon system in the presence of the piezoelectric effect looks like:

$$\hat{H} = \hat{H}_e + \hat{H}_{ac} + \hat{H}_{e-pz}. \tag{59}$$

We will take into account only the levels of the stationary electronic spectrum. Then, to perform their renormalization by the interaction with acoustic phonons due to the piezoelectric potential, one should perform the Fourier transform for the Green's function obtained from the Dyson equation [10, 21]:

$$G_n(\Omega) = \left(\Omega - E_{n\bar{k}} - M_n(\Omega) \right)^{-1}. \tag{60}$$

Having applied the one-phonon approximation, we represent the mass operator in the Dyson equation as follows:

$$M_n(\Omega, \bar{k}) = \sum_{q n_1 n'} \left| F_{nn_1n'}(q) \right|^2 \left[\frac{1 + \nu_{n_1}}{\Omega - E_{n', \bar{k}+\bar{q}} - \hbar\omega_{n_1} + i\eta} + \frac{\nu_{n_1}}{\Omega - E_{n', \bar{k}+\bar{q}} + \hbar\omega_{n_1} + i\eta} \right],\ \eta \to \pm 0, \tag{61}$$

where $\nu_{n_1} = (e^{\hbar\omega_{n_1}/k_B T} - 1)^{-1}$ is the occupation number for acoustic phonon modes.

In the available nanodevices the electron flow is directed in such a way, that it moves almost strictly along the axis Oz, perpendicular to the layers of the nanostructure. The value $\bar{k} = 0$ satisfies this case, then we obtain that according to (51) $\Omega = E_n$. The interaction of electrons with acoustic phonons due to the piezoelectric potential is determined

by the renormalized value of the energy of the electronic spectrum $\tilde{E}_n$, which, in turn, are characterized by temperature shifts (Δ_n) and decay rates (Γ_n). The latter quantities were obtained from the poles of the Fourier transform for the Green's function (60).

Because of that we have

$$M_n(\Omega = E_n, \bar{k} = 0) = \Delta_n - i\frac{\Gamma_n}{2}, \tag{62}$$

then the solutions of the dispersion equation

$$E_n - E_{n,\bar{q}} - M_n(\Omega = E_n, \bar{k} = 0) = 0 \tag{63}$$

are as follows:

$$\begin{aligned}
\Delta_n &= \operatorname{Re} M_n(\Omega = E_n, \bar{k} = 0) = \frac{\Delta l_x \Delta l_y}{4\pi^2} \sum_{n_1,\pm} \left(\nu_{n_1} + \frac{1}{2} \pm \frac{1}{2} \right) \mathrm{P} \iint \left(E_n - E_{n,\bar{q}} \mp \Omega_{n_1} \right)^{-1} \left| F_{nn_1n}(q) \right|^2 d^2 q, \\
\Gamma_n &= -2 \operatorname{Im} M_n(\Omega = E_n, \bar{k} = 0) = \frac{\Delta l_x \Delta l_y}{2\pi} \sum_{n_1,\pm} \left(\nu_{n_1} + \frac{1}{2} \pm \frac{1}{2} \right) \iint \delta\left(E_n - E_{n,\bar{q}} \mp \Omega_{n_1} \right)^{-1} \left| F_{nn_1n}(q) \right|^2 d^2 q,
\end{aligned} \tag{64}$$

where the first integral in expressions (64) is taken in the sense of the principal Cauchy value.

4. Discussion of the results

The direct calculations based on the theory developed in Secs. (2) and (3) were performed using the example of a two-well (width of the potential wells $w_1 = w_2 = 5$ nm, the thickness of the barriers $b_1 = b_2 = b_3 = 2$ nm, the nanostructure cross-sectional area parameters are $\Delta l_x = \Delta l_y = 10^{-5}$ nm) nanostructure with the physical parameters, which are taken from papers [15, 18–20, 22], given in Table 1.

In Fig. 2(a) the results of calculating the dependences of the shear acoustic phonons spectrum on the wave vector are shown. As can be seen from the figure, the shear acoustic phonons spectrum $\Omega_{n_1}(q)$ in the presence of the piezoelectric effect consists of a set of dependences branches, which are located in the range from $\Omega_2'(q)$ to $\Omega_1'(q)$, and these boundaries are determined by solutions of the equation, which follows from the relation (21):

$$\left(q^2 e_{15}^{(p)} \right)^2 + \varepsilon_\infty^{(p)} q^2 \frac{\left(q^2 C_{44}^{(p)} - \rho^{(p)} \omega^2 \right) \left(\omega^2 - \left(\omega_{LO(E_1)}^{(p)} \right)^2 \right)}{\omega^2 - \left(\omega_{TO(E_1)}^{(p)} \right)^2} = 0 \tag{65}$$

and the conditions imposed on the possible values of the acoustic phonons energies [23]:

$$\Omega_{ac}(q) \le 25 - 30 \text{ meV}, \tag{66}$$

which, determines the values of $\Omega_1'(q)$ and $\Omega_2'(q)$, respectively, rejecting the values $\omega(q)$, that do not satisfy condition (66).

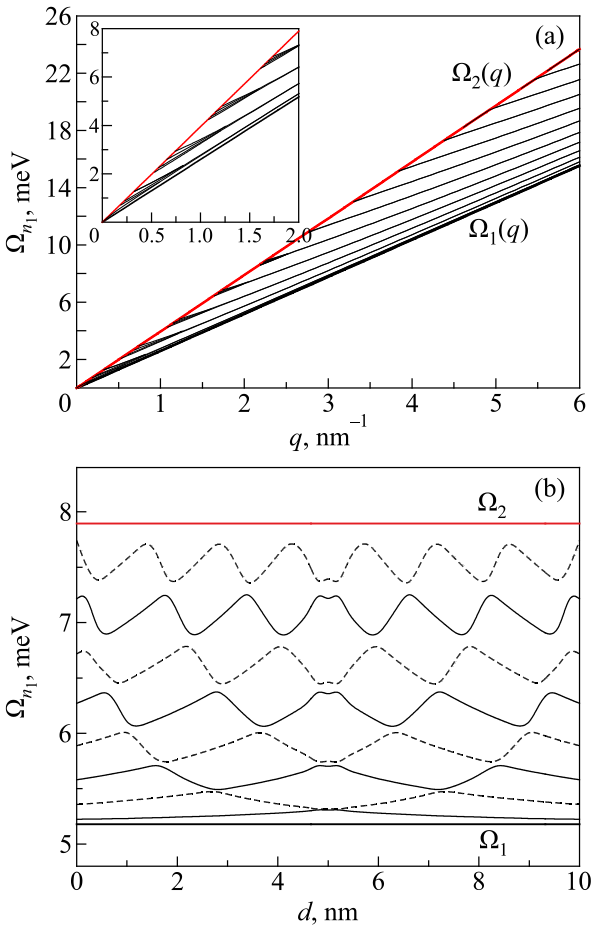

Fig. 2. Dependences of the shear acoustic phonons spectrum on the wave vector q (a) and on the total width of the potential well ($0 \le d \le d_1 + d_2$) (b) at $q = 24/z_3$.

Table 1. Physical parameters of the AlN/GaN nanostructure materials

	m/m_e	ε_∞	P, kg/m^3	C_{44}, GPa	e_{15}, C/m^2	P_{Sp}, C/m^2
GaN	0.186	10	6150	105	0.33	–0.029
AlN	0.322	8.5	3255	116	–0.42	–0.081
	$\omega_{LO(E_1)}$, meV		$\omega_{TO(E_1)}$, meV	$\omega_{LO(A_1)}$, meV		$\omega_{TO(A_1)}$, meV
GaN	91.83		69.25	90.97		65.91
AlN	113.02		83.13	110.3		75.72

The calculated dependences $\Omega_{n_1}(q)$ are formed at the corresponding values $\Omega'_2(q)$ and increase quasilinearly, exhibiting insignificant quadratic tendencies with a small change in the value of q near the point of their formation. The main feature of the spectrum dependences $\Omega_{n_1}(q)$ is that, firstly, for each group of branches, four branches of dependences are first formed, two of which each with different variance on q. With the increase of q values, as it can be seen from the footnote in Fig. 2(a), two branches with the same dispersion first approach and merge are formed, and then these branches also merge — one branch is formed, the energy values in which slowly approach the dependence $\Omega'_1(q)$.

It should be noted, that the following effect is available for each of the formed branches: with an increase of the number n_1, the distance between the adjacent branches of acoustic phonon energies increases.

Further, in Fig. 2(b) the dependences of the shear acoustic phonons spectrum on the value of the total potential well $(0 \le d \le d_1 + d_2)$ are shown. It can be seen from the figure that in the calculated dependences for the first branches, n_1 maxima and n_1-1 minima are clearly formed, respectively,

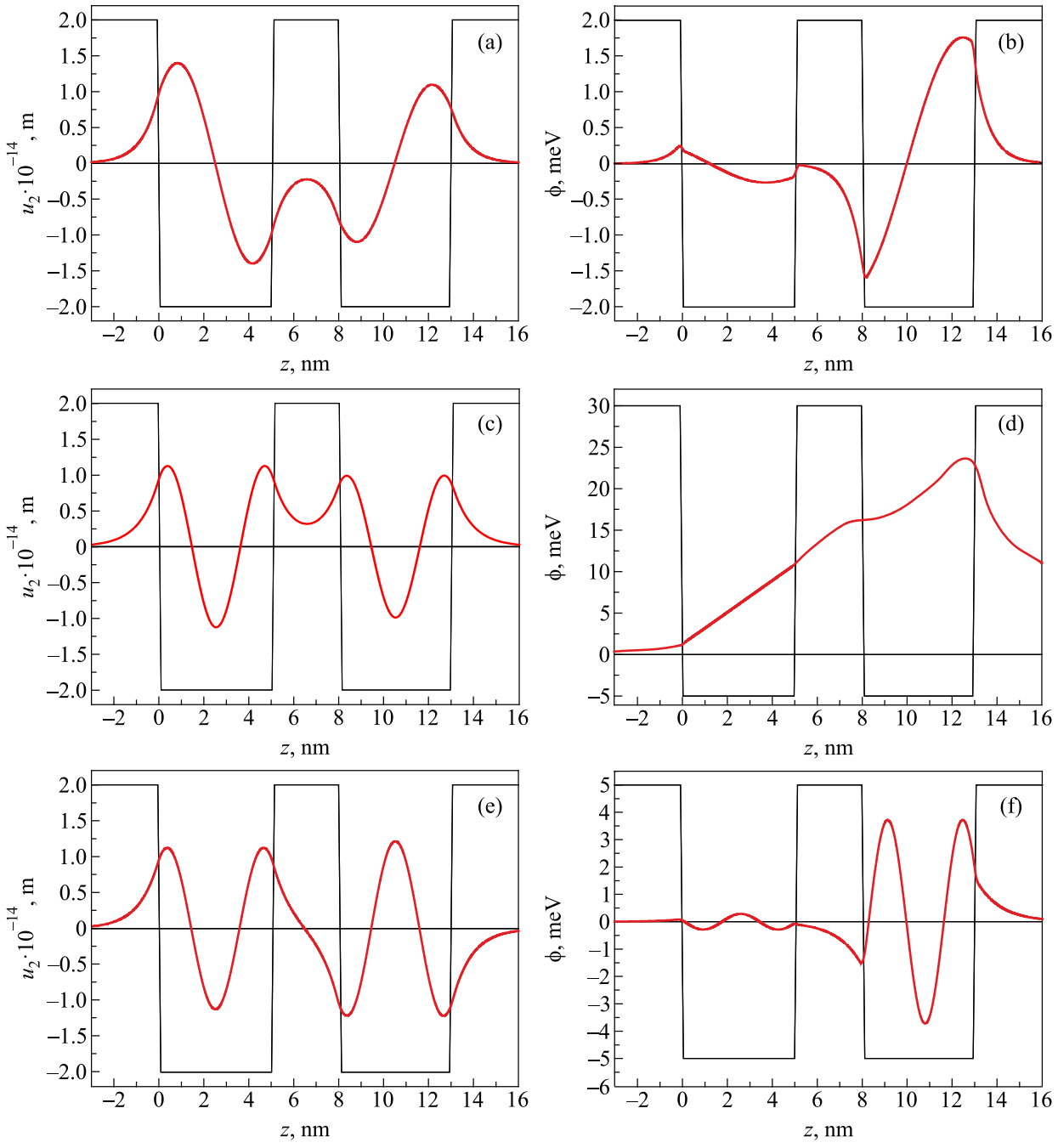

Fig. 3. Dependences of the elastic displacement $u_2(z)$ (a), (c), and (e) and potential $\phi(z)$ (b), (d), and (f) calculated at $q = 24/z_3$ for the acoustic phonons energies: 5.312, 6.401, and 7.287 meV.

for each branch. Next, for each of the branches $\Omega_{n_1}(d)$, there are n_1+1 maxima and n_1 minima. Besides, we observe an weakly expressed extrema (minima for odd values of n_1 and maxima for even values of n_1), which is located in the vicinity of the point corresponding to the symmetric position of the internal potential barrier [$d \to (d_1 + d_2)/2$].

In Figs. 3(a)–3(f) the examples of the elastic displacement $u_2(z)$ and the potential $\varphi(z)$ dependences on z, calculated for a fixed value of q and the corresponding values of the energies of acoustic phonons $\hbar\omega_q$ are shown. As can seen from Figs. 3(a), 3(c), and 3(e), the dependences of the elastic displacement $u_2(z)$ can behave differently in different the nanostructure layers. So, in the left and right potential barriers and the external semiconductor medium, in accordance with relation (26), the displacement values follow to zero while acquiring positive values, as can be seen from Figs. 3(a) and 3(c), or acquiring negative values in the medium to the right of the nanostructure as in Fig. 3(e). The established effect does not take place in the dependences for the potentials shown in Figs. 3(b), 3(d), and 3(f).

It should be noted, that in the potential wells the elastic displacement dependences behave as antisymmetric functions relative to the center of these nanostructure layers [Fig. 3(a)] or symmetric functions relative to this point [Figs. 3(c) and 3(e)]. For such cases, the corresponding dependences for the potentials [Figs. 3(b) and 3(d)]: in the first case, the potential first decreases from left to right and increases further, and in the second case it increases practically over the entire region of the nanostructure. For the case in Figs. 3(e) and 3(f) we reveal, that the maxima of the function $u_2(z)$ correspond to the minima of the function $\varphi(z)$ and vice versa.

If the maxima [Fig. 3(a)] or minima [Fig. 3(b)] of the function $u_2(z)$ is formed in the layer corresponding to the internal barrier of the nanostructure, then the dependence $\varphi(z)$ in this region decreases [Fig. 3(b)] and increases [Fig. 3(d)] correspondingly. For the case in Figs. 3(e) and 3(f) both functions $u_2(z)$ and $\varphi(z)$ decrease in the region of the inner barrier.

In Fig. 4 the dependences for the first four electronic levels of the investigated nanostructure, calculated at room temperature (T = 300 K), on the position of the internal potential barrier in the total potential well (d) are shown. As can be seen in the figure the calculated dependences are specified by the presence of n maxima and n-1 minima for each number of the energy level n. It must be noted, that the formation of anticrossings for the dependences of the nearest energy levels takes place. In addition, the dependences $E_n(d)$ lack their symmetry relative to the symmetric position of the internal potential barrier, which is due to the presence of strong internal electric fields, according to relation (39).

In Figs. 5(a)–5(h) the results of calculation the values of the stationary electronic spectrum level shifts and their decay rates at different temperatures are shown as the dependence of the internal potential barrier position in

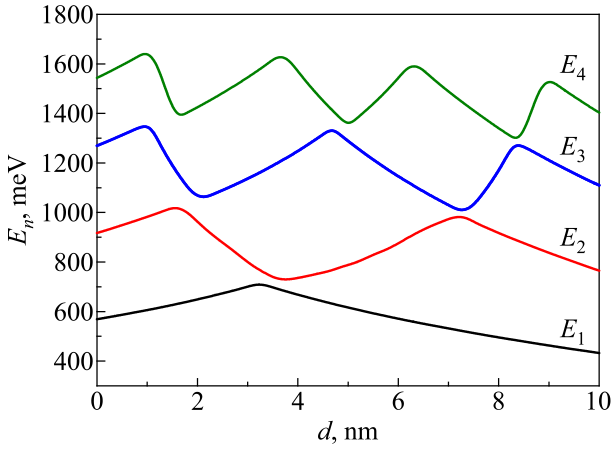

Fig. 4. Dependences of the first four levels of the electronic spectrum on the total potential well width ($0 \le d \le d_1 + d_2$) at T = 300 K.

the total potential well. To clarity the obtained results, all calculations were performed for temperature values ranging from 0 K (the most obvious case) to 300 K (room temperature case) with an increment of 100 K, covering the value of 100 K (corresponds to the temperature range for the operation of nanodevices, in which liquid nitrogen cooling is used). As can be seen from Figs. 5(a), 5(c), 5(e), and 5(g), the values of the electronic spectrum level shifts, depending on the value of d, take the values having both positive and negative signs, which is not observed in the case of interaction of electrons with flexural and dilatational acoustic phonons [10] (in this case, the temperature shift is always negative). This effect is determined by the properties of symmetry and the sign of the functions $\phi^{(p)}(q, \omega_{n_1 q}, z)$ included in relation (64). It should be noted, that in most configurations of the nanostructure total potential well, the absolute values of the shifts $\Delta_n(d)$ increase with the temperature increasing, and there is no correlation between the maximum value of the temperature shift and the number of the electronic level n. With an increase of temperature, the dependence obtained at T = 0 K is deformed, the extrema formed with a change in d being more sufficient, acquiring larger absolute values, their position changes slightly. As it can be seen from the above dependences, there is a regularity for temperatures shifts $\Delta_n(d)$, relatively the symmetric position of the internal potential barrier ($d \to (d_1 + d_2)/2$). At this point, a minimum belonging to the interval, in which the shift of the level is negative in all dependences is formed. The width of this interval decreases with the increase of the electronic level number n. To the left and right of the mentioned interval, two intervals with the positive values of energy levels shifts are formed. This shift becomes significant with the increase of temperature for all levels, except for level n = 3. In this case, the intervals with the positive shifts are the most (width about 1.5 nm), but the shifts increase slightly with the increase of temperature, reaching maximum values at the end of these intervals.

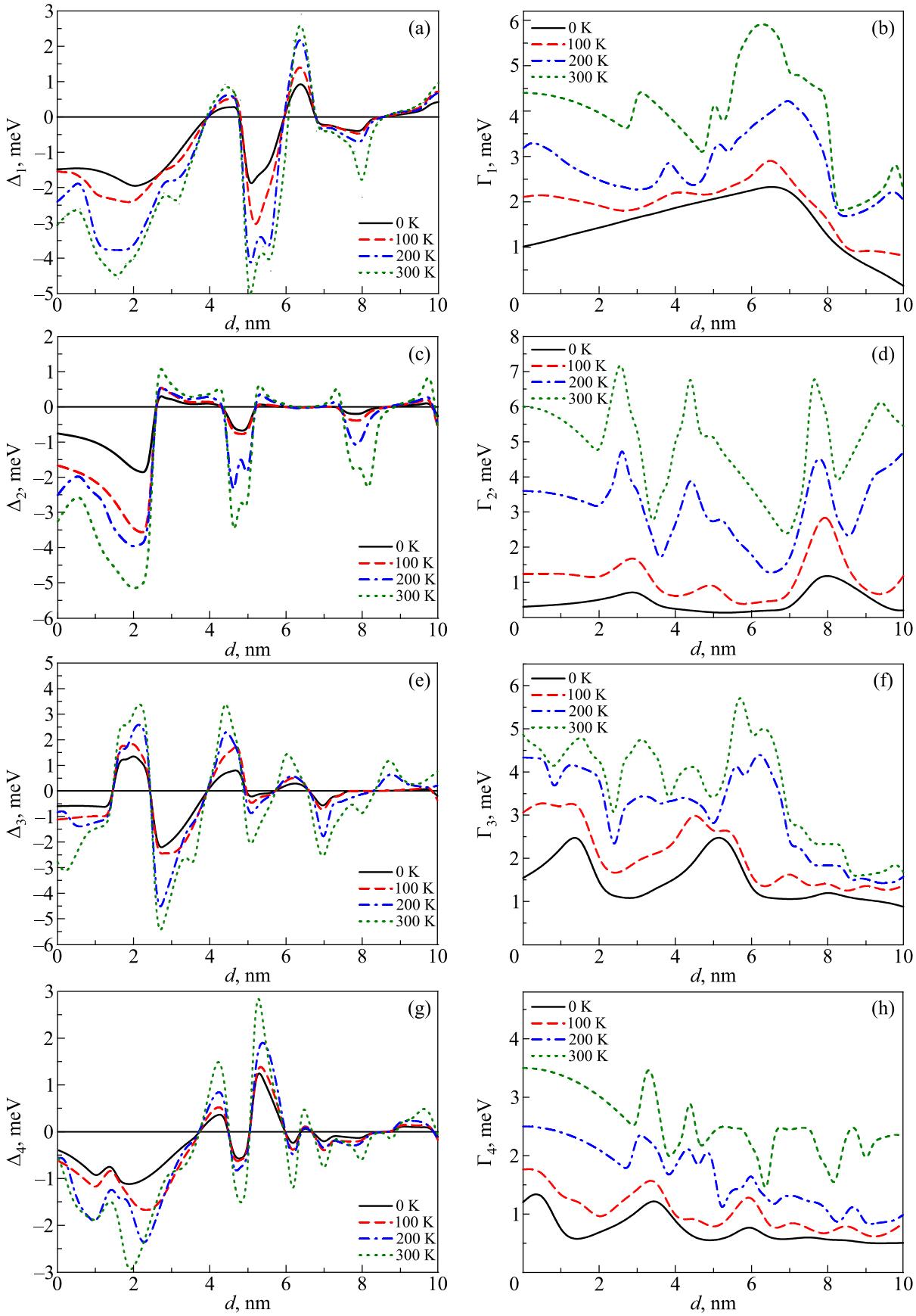

Fig. 5. (Color online) Dependences of the shifts for the first ($n = 4$) levels of the electronic spectrum and their decay rates on the total width of the potential well d ($0 \le d \le d_1 + d_2$) (b) at $q = 24/z_3$, calculated for various values of the temperature T: 0 K (black solid line), 100 K (red dashed line), 200 K (blue dash-dotted line), 300 K (green dotted line).

Besides the energy levels shifts at small sizes of the left potential well [interval $0-(d_1+d_2)/3$] is significant at $n = 3$, changing its sign in this interval and forming a positive maximum. In general, it should be concluded, that in the regions at $d > (d_1+d_2)/2$ (for the larger left potential well) the magnitude of the temperature shifts is smaller than at $d < (d_1+d_2)/2$.

Further, in Figs. 5(b), 5(d), 5(f), and 5(h), the dependences on the value of d for the decay rates of electronic states calculated for the same temperature values as the temperature shifts, are shown. As can be seen from the given dependences for $\Gamma_n(d)$ at $T = 0$ K, they form a number of maxima equal to the number of the electronic level n, and, accordingly, n–1 minima. As the values of temperature T increase, so do the values of the decay rates for the electronic levels: if at a temperature of 100 K these values increase by 1.5–2 times, and at a temperature of 300 K by 5–6 times. It should be noted that extrema in the dependences $\Gamma_n(d)$ arising at $T = 0$ K are also presented at 100, 200, and 300 K, but there is a gradual deformation of these dependences with the emergence of new extrema. This effect mostly arises for the third ($n = 3$) and fourth ($n = 4$) electronic levels. For the first two electronic levels, the deformation of the $\Gamma_n(d)$ dependences is relatively insignificant.

To sum up, it should be concluded, that the interaction of electrons with acoustic phonons due to the piezoelectric potential results in the renormalization of the electronic spectrum levels, thus directly affecting the energy of electronic transitions $\Omega_{nm} = E_m - E_n$, $n \neq m$. In this case, the renormalization of the absorption band $\Gamma_{nm} = \Gamma_m + \Gamma_n$, $n \neq m$ (for electronic transitions with detection of the electromagnetic field energy) or the laser radiation band (for laser quantum transitions) also occurs. With the increase of temperature, the expansion $\Delta\Gamma_{nm} = \Delta\Gamma_{nm}(T) - \Delta\Gamma_{nm}(0)$ of these bands increases, which requires practical investigation of such effects.

Conclusions

An analytical theory of the interaction of electrons with shear acoustic phonons due to the created by them piezoelectric potential for arbitrary values of temperature is developed.

Using the method of Green's functions and the Dyson equation, expressions that describe the temperature shifts of the electronic levels of the nanostructure and their decay rates were established.

Calculations of the electrons spectrum, spectrum of the acoustic phonons, and the potential caused by them have been performed using the physical parameters of the double-well AlN/GaN nanostructure.

Results of direct calculations of the temperature shifts for electronic levels and their decay rates have shown, that the increase of temperature to values close to the room temperature makes it necessary to take into account the renormalization of the energies of quantum electronic transitions and expansion of the bands of absorption or laser radiation.

1. P. M. Mensz, B. Dror, A. Ajay, C. Bougerol, E. Monroy, M. Orenstein, and G. Bahir, *J. Appl. Phys.* **125**, 174505 (2019).
2. A. Ishida, K. Matsue, Y. Inoue, H. Fujiyasu, H.-Ju. Ko, A. Setiawan, J.-J. Kim, H. Makino, and T. Yao, *J. Appl. Phys. Jpn*. **44**, 5918 (2005).
3. B. K. Ridley, W. J. Schaff, and L. F. Eastman, *J. Appl. Phys.* **94**, 3972 (2003).
4. F. Bernardini, V. Fiorentini, and D. Vanderbilt, *Phys. Rev. B* **56**, R10024(R) (1997).
5. F. Bernardini and V. Fiorentini, *Phys. Status Solidi B* **216**, 391 (1999).
6. F. Bernardini and V. Fiorentini, *Phys. Rev. B* **57**, R9427(R) (1998).
7. S. Saha and J. Kumar, *J. Comput. Electron*. **15**, 1531 (2016).
8. I. V. Boyko, *Condens. Matter Phys*. **21**, 43701 (2018).
9. I. Boyko, M. Petryk, and J. Fraissard, *Eur. Phys. J. B* **93**, 67 (2020).
10. I. V. Boyko and M. R. Petryk, *Condens. Matter Phys.* **23**, 33708 (2020).
11. E. P. Pokatilov, D. L. Nika, and A. A. Balandin, *Superlatt. Microstruct.* **33**, 155 (2003).
12. P. D. Sesion, Jr., E. L. Albuquerque, M. S. Vasconcelos, P. W. Mauriz, and V. N. Freire, *Eur. Phys. J. B* **51**, 583 (2006).
13. P. D. Sesion, Jr., E. L. Albuquerque, C. Chesman, and V. N. Freire, *Eur. Phys. J. B* **58**, 379 (2007).
14. M. A. Stroscio and M. Dutta, *Phonons in Nanostructures*, Cambridge University Press, Cambridge (2001).
15. J. Piprek, *Nitride Semiconductor Devices: Principles and Simulation*, Wiley-VCH, Weinheim (2007).
16. S. Leconte, F. Guillot, E. Sarigiannidou, and E. Monroy, *Semicond. Sci. Technol.* **22**, 107 (2006).
17. X. Gao, D. Botez, and I. Knezevic, *J. Appl. Phys.* **101**, 063101 (2007).
18. J.-M. Wagner and F. Bechstedt, *Phys. Rev. B* **66**, 115202 (2002).
19. Q. Yan, P. Rinke, M. Scheffler, and C. G. Van de Walle, *J. Appl. Phys.* **195**, 121111 (2009).
20. Q. Yan, P. Rinke, A. Janotti, M. Scheffler, and C. G. Van de Walle, *Phys. Rev. B* **90**, 125118 (2014).
21. M. V. Tkach, Ju. O. Seti, Y. B. Grynyshyn, and O. M. Voitsekhivska, *Condens. Matter Phys.* **17**, 23704 (2014).
22. B. K. Sahoo, *J. Mater. Sci*. **47**, 2624 (2011).
23. C. Bungaro, K. Rapcewicz, and J. Bernholc, *Phys. Rev. B* **61**, 6720 (2000).

Теорія спектру поперечних акустичних фононів та їх взаємодії з електронами через п'єзоелектричний потенціал у AlN/GaN наноструктурах плоскої симетрії

I. V. Boyko, M. R. Petryk, J. Fraissard

З використанням моделей пружного та діелектричного континууму отримано систему диференціальних рівнянь, знайдені точні аналітичні розв'язки якої описують пружне зміщення середовища нітридної напівпровідникової наноструктури та п'єзоелектричний ефект, який зумовлений поперечними акустичними фононами. Розвинено теорію спектру поперечних акустичних фононів та пов'язаного з ними п'єзоелектричного потенціалу. Показано, що поперечні акустичні фонони не взаємодіють з електронами через деформаційний потенціал, проте така взаємодія може відбуватися через п'єзоелектричний потенціал. За допомогою методу температурних функцій Гріна та рівняння Дайсона отримано вирази, які описують температурні залежності зміщень рівнів електронного спектру та їх згасання. Розрахунки спектру електронів, акустичних фононів та характеристик, що визначають їх взаємодію при різних температурах, виконувались на прикладі фізичних та геометричних параметрів типової AlN/GaN наноструктури, що може бути елементом окремого каскаду квантового каскадного лазера чи детектора.

Ключові слова: акустичний фонон, напівпровідник на основі нітриду, п'єзоелектричний ефект, рівняння Дайсона, функція Гріна.